Electrocatalysis

International Edition: DOI: 10.1002/anie.201508490
German Edition: DOI: 10.1002/ange.201508490

Activating a Low Overpotential CO_2 Reduction Mechanism by a Strategic Ligand Modification on a Ruthenium Polypyridyl Catalyst

*Ben A. Johnson[+], Somnath Maji[+], Hemlata Agarwala, Travis A. White, Edgar Mijangos, and Sascha Ott**

Abstract: *The introduction of a simple methyl substituent on the bipyridine ligand of $[Ru(tBu_3tpy)(bpy)(NCCH_3)]^{2+}$ (tBu_3tpy = 4,4′,4″-tri-tert-butyl-2,2′:6′,2″-terpyridine; bpy = 2,2′-bipyridine) gives rise to a highly active electrocatalyst for the reduction of CO_2 to CO. The methyl group enables CO_2 binding already at the one-electron reduced state of the complex to enter a previously not accessible catalytic cycle that operates at the potential of the first reduction. The complex turns over with a Faradaic efficiency close to unity and at an overpotential that is amongst the lowest ever reported for homogenous CO_2 reduction catalysts.*

Molecular systems for electrochemical CO_2 reduction often operate at high overpotentials, making the transition to large-scale production of liquid fuels or high-value C_n products from CO_2 inefficient and unfeasible.[1] Developing a low overpotential electrocatalyst for CO_2 reduction would inevitably alter the economics of producing renewable, carbon-neutral fuels from anthropogenic CO_2.[2] Owing to the fact that CO_2 reduction products, such as CO, can be immediately utilized within the existing energy infrastructure using the Fischer–Tropsch process for gas-to-liquid fuel conversion,[3] such a strategy is highly advantageous and merits further exploration.

Electrocatalytic processes operate efficiently when the effective overpotential, η, defined by the difference between the potential for catalysis at half the maximum catalytic current ($E_{cat/2}$) and the thermodynamic potential of the reaction (E^o_{rxn}),[4] is minimized. When multiple oxidation/reduction events are required for a particular reaction, the accumulation of redox equivalents on a single molecular catalyst makes subsequent oxidation/reduction processes energetically more demanding. Charge equilibration is necessary to counterbalance introduced charge and to facilitate further oxidations/reductions at a milder potential, preferably at the same potential as the previous step. Natural systems display elegant examples of decreasing overpotential with charge compensation. In [FeFe]-hydrogenase enzymes, protonation of the $[Fe_2S_2]$ subcluster is critical to efficiently accumulate reducing equivalents for proton reduction within a narrow potential window.[5] The water oxidation complex in photosystem II offers an extreme example where the four consecutive oxidations of the $CaMn_4$ cluster occur over a range of only about 0.3 V. This is only possible because of the release of protons to compensate for the charge build-up.[6]

In synthetic catalysts, the strategy to compress the potential window for multiple oxidations or reductions is well-known for water oxidation[7] and proton reduction,[8] but less explored for CO_2 reduction.[9] Although some catalysts bind CO_2 already at the one-electron reduced state,[2f,10] many of the more active and selective catalysts enter catalysis only after an initial two-fold reduction. This necessity to reduce the catalyst twice without any charge compensation step leads to increased overpotentials. Examples of these types of catalysts are $[Re^I(bpy)(CO)_3Cl]$ and $[Mn^I(bpy)(CO)_3Cl]$ (bpy = 2,2′-bipyridine),[11] and polypyridyl-based catalysts such as $[Ru(tpy)(bpy)S]^{2+}$ (tpy = 2,2′:6′,2″-terpyridine, S = solvent).[12] With the latter system, we have recently demonstrated that raising the electron-donor capacity of the bpy ligand enhances the lability of the monodentate ligand and facilitates catalysis.[13] In the present study, we show that a simple methyl substituent in the 6 position of the bpy ligand activates the mono-reduced Ru catalyst. This effect is demonstrated by comparing the voltammetric response of $[Ru(tBu_3tpy)(4,4'\text{-dmbpy})(NCCH_3)]^{2+}$ ($\mathbf{1}^{2+}$; tBu_3tpy = 4,4′,4″-tri-*tert*-butyl-2,2′:6′,2″-terpyridine, 4,4′-dmbpy = 4,4′-dimethyl-2,2′-bipyridine) with that of $[Ru(tBu_3tpy)(6\text{-mbpy})(NCCH_3)]^{2+}$ ($\mathbf{2}^{2+}$; 6-mbpy = 6-methyl-2,2′-bipyridine; Scheme 1) in the presence of CO_2. CO_2 binding occurs already at the one-electron reduced form of $\mathbf{2}^{2+}$, and enables a second electron uptake at the same potential. The achieved compression of reduction potentials, which used to be consecutive but now appear in one electrochemical process, leads to a significantly decreased overpotential for catalysis.

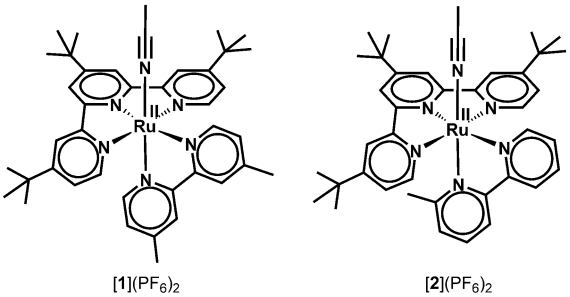

[1](PF6)2 [2](PF6)2

Scheme 1. Structures of complexes $\mathbf{1}(PF_6)_2$ and $\mathbf{2}(PF_6)_2$.

[*] B. A. Johnson,[+] Dr. S. Maji,[+] Dr. H. Agarwala, Dr. T. A. White, Dr. E. Mijangos, Prof. Dr. S. Ott
Department of Chemistry
Ångström Laboratory, Uppsala University
Box 523, 75120 Uppsala (Sweden)
E-mail: sascha.ott@kemi.uu.se

[+] These authors contributed equally to this work.

Supporting information for this article is available on the WWW under http://dx.doi.org/10.1002/anie.201508490.

The synthesis of $\mathbf{1}^{2+}$ and $\mathbf{2}^{2+}$ (Scheme 1) was accomplished in a stepwise manner by first reacting $RuCl_3 \cdot 3H_2O$ with tBu$_3$tpy to form [Ru(tBu$_3$tpy)Cl$_3$], followed by treatment with the substituted bpy (NN; where NN = 6-mbpy or 4,4′-dmdpy) to yield [Ru(tBu$_3$tpy)(NN)Cl]$^{1+}$. The chloride can easily be exchanged for CH_3CN by refluxing the complexes in a H_2O/CH_3CN mixture, affording the final products, [Ru(tBu$_3$tpy)(NN)(NCCH$_3$)]$^{2+}$, as orange solids. Complex $\mathbf{2}^{2+}$ was identified as the isomer in which the methyl-substituted ring of the 6-mbpy ligand is *trans* to the CH_3CN ligand, based on 2D COSY NMR spectroscopy (see Figure S1 in the Supporting Information) to assign all protons of the spectrum, combined with a 1D difference NOE experiment (Figure S3, Supporting Information). Further characterization of the complexes and detailed synthetic procedures are described in the Supporting Information.

Cyclic voltammograms (CVs) of $\mathbf{1}^{2+}$ and $\mathbf{2}^{2+}$ in Ar-purged CH_3CN solutions using 0.1 M Bu_4NPF_6 as the supporting electrolyte are shown in Figure 1. On the anodic scan, reversible waves can be detected at 0.77 and 0.83 V versus $Fc^{+/0}$ for $\mathbf{1}^{2+}$ and $\mathbf{2}^{2+}$, respectively. In analogy to previous reports,[14] this couple can be assigned to a metal-based $Ru^{3+/2+}$ oxidation, which is consistent with density function theory (DFT) calculations (Figure S4). The lower potential of

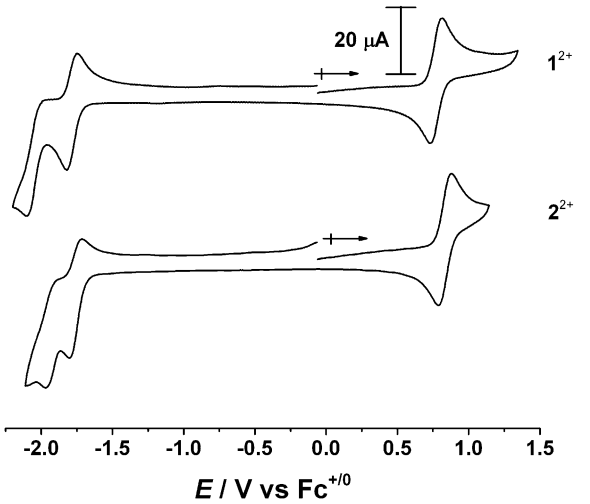

Figure 1. Cyclic voltammograms of [Ru(tBu$_3$tpy)(NN)(NCCH$_3$)]$^{2+}$ complexes $\mathbf{1}^{2+}$ (top) and $\mathbf{2}^{2+}$ (bottom), 1 mM in Ar-purged CH_3CN with 0.1 M Bu_4NPF_6 as the supporting electrolyte at a scan rate $\nu = 200\ mV\,s^{-1}$.

$\mathbf{1}^{2+}$ as compared to $\mathbf{2}^{2+}$ reflects the slightly increased electron-donating character of 4,4′-dmbpy as compared to 6-mbpy. The cathodic scans (scan rate $\nu = 200\ mV\,s^{-1}$) show a reversible couple at $E_{1/2} = -1.78$ V and -1.76 V for $\mathbf{1}^{2+}$ and $\mathbf{2}^{2+}$, respectively, followed by a second irreversible reduction ($E_{p,c} = -2.09$ V and -1.98 V for $\mathbf{1}^{2+}$ and $\mathbf{2}^{2+}$, respectively). Results from DFT calculations indicate that the first reduction occurs on tBu$_3$tpy, forming [Ru(tBu$_3$tpy$^{\bullet-}$)(NN)(NCCH$_3$)]$^{+}$, and the second reduction is bpy-based to yield the two-electron reduced complex [Ru(tBu$_3$tpy$^{\bullet-}$)(NN$^{\bullet-}$)(NCCH$_3$)]^{0} (Figure S4). The irreversibility of the second reduction at 200 mV s^{-1} is caused by the loss of the CH_3CN ligand following the two one-electron reduction processes.

CVs with varying scan rates (25 mV s^{-1} to 2000 mV s^{-1}) under an Ar atmosphere for the first and second reduction of $\mathbf{1}^{2+}$ and $\mathbf{2}^{2+}$ (Figure S5) reveal that the reversibility of these processes are dependent on scan rate. The first reduction couple of $\mathbf{1}^{2+}$ at -1.78 V is reversible at all scan rates, whereas the second reduction of $\mathbf{1}^{2+}$ at -2.09 V is irreversible at 200 mV s^{-1} but becomes reversible at scan rates above 1000 mV s^{-1}. In contrast, the second reduction for $\mathbf{2}^{2+}$ shows complete irreversibility at -1.98 V up to 2000 mV s^{-1}, which indicates that CH_3CN dissociation in $\mathbf{2}^{2+}$ occurs with more rapid kinetics than in $\mathbf{1}^{2+}$. This behavior is explained by the steric demand from the *ortho* methyl substituent in $\mathbf{2}^{2+}$ that tilts the bpy ligand towards the coordinated CH_3CN, resulting in enhanced lability of the acetonitrile ligand compared to the situation in $\mathbf{1}^{2+}$. The behavior is consistent with a recent report by Turro and co-workers who observed a 1000-fold increase in pyridine (py) photodissociation upon introduction of methyl substituents in the 6 position of the bpy in [Ru(tpy)(bpy)(py)]$^{2+}$.[15]

In CO_2-saturated CH_3CN solutions, the cyclic voltammograms of $\mathbf{1}^{2+}$ and $\mathbf{2}^{2+}$ show typical current enhancement corresponding to electrocatalytic CO_2 reduction at potentials beyond -2 V (Figure 2). Both complexes thus display the previously reported CO_2 reduction reactivity,[12a] that is, an EEC mechanism (electron transfer, electron transfer, chemical reaction) in which two ligand-based reductions are followed by CH_3CN dissociation and CO_2 binding to yield the two-electron reduced CO_2 adduct [Ru(tBu$_3$tpy)(NN)(CO_2^{2-})]^{0} (Scheme 2 A). A closer look at the first reduction processes in the CVs of $\mathbf{1}^{2+}$ and $\mathbf{2}^{2+}$ under CO_2 however reveals a striking difference. The first reduction of $\mathbf{1}^{2+}$ is reversible under CO_2, and the potential is unchanged from the CV under Ar (inset in Figure 2 A). Conversely, this first reduction for $\mathbf{2}^{2+}$ under CO_2 is irreversible and shows current enhancement.

The peak potential ($E_{p,c}$) of the wave under CO_2 is shifted to more positive potentials compared to that detected in the CV under Ar (Figure 2 B, inset). When measured at 25 mV s^{-1}, $E_{p,c}$ is shifted by a maximum of + 33 mV, indicative of a chemical reaction subsequent to the electron transfer. As this effect is only evident under CO_2, it is clear that this chemical reaction is the formation of the metal-bound CO_2 adduct. DFT calculations show that CO_2 binding is concomitant with charge redistribution from the initially reduced tBu$_3$tpy ligand to CO_2, and the produced species is best described as [Ru(tBu$_3$tpy)(6-mbpy)($CO_2^{\bullet-}$)]$^{+}$ with the negative charge being largely localized on the metal-bound CO_2 (Figure S6). The charge redistribution enables a second reduction at the same or more positive potential, as evidenced by the increased current at -1.82 V (Figure 2 B, inset), to generate the catalytically active metallocarboxylate complex [Ru(tBu$_3$tpy)(6-mbpy)(CO_2^{2-})]^{0}. The steric effect of a simple methyl substituent has thus opened a new mechanistic pathway in which the order of electrochemical and chemical events is changed from EEC to ECE (Scheme 2 B).

Previous studies have demonstrated that complexes of type [Ru(tpy)(bpy)S]$^{2+}$ (S = solvent) that follow the EEC

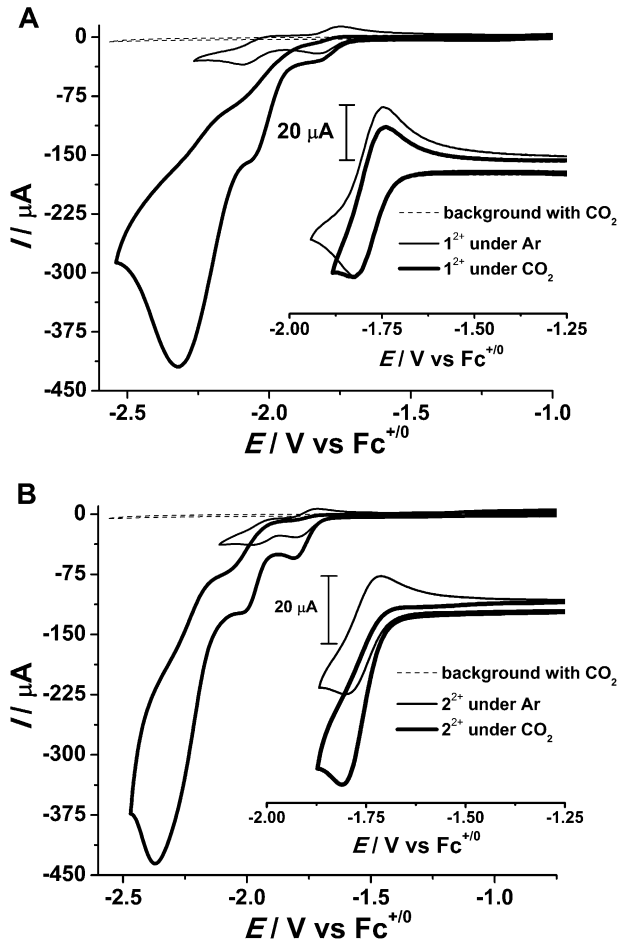

Figure 2. Cyclic voltammograms of 1 mM solutions of A) $\mathbf{1}^{2+}$ and B) $\mathbf{2}^{2+}$ under Ar and CO_2 atmospheres at a scan rate of 200 $mV s^{-1}$. Insets: expansion of the first reduction process for each complex under Ar and CO_2 atmospheres. All measurements were performed in CH_3CN with 0.1 M Bu_4NPF_6 as the supporting electrolyte.

mechanism produce CO by means of the reductive disproportionation of CO_2. With CO_2 not only being the substrate but also the oxide acceptor, CO_3^{2-} (or its protonated form HCO_3^-) is produced as a byproduct.[12a,b,16] Controlled potential electrolysis experiments were performed to confirm catalytic turnover at the potential of the first reduction of $\mathbf{2}^{2+}$ by monitoring the formation of the reduction products, CO and CO_3^{2-}, by gas chromatography (GC) and IR spectroscopy, respectively. Thus, a 1 mM solution of $\mathbf{2}^{2+}$ in CH_3CN was held at the first reduction potential (−1.82 V versus $Fc^{+/0}$). GC analysis showed CO as the exclusive gaseous product; specifically H_2 was not detected during the experiment. A ^1H NMR spectrum after the bulk electrolysis confirmed the absence of $HCOO^-$ (Figure S7). During the controlled potential electrolysis, aliquots of the solution were taken at ten-minute intervals and analyzed by IR spectroscopy (Figure 3). The appearance of three bands at 1684 cm^{-1}, 1645 cm^{-1}, and 1305 cm^{-1} can be assigned to the formation of free bicarbonate in solution.[17] The increase in the intensity of these bands with increasing time during the experiment supports the conclusion that catalysis occurs at the first reduction potential of $\mathbf{2}^{2+}$. Quantification of the amount of produced HCO_3^- by IR spectroscopy (Figure S8) allows determination of the Faradaic efficiency for the reductive disproportionation of CO_2 to CO and CO_3^{2-} catalyzed by $\mathbf{2}^{2+}$ as having a value of 94.7 %. Electrocatalysis is sustained with a current density of 1.33 mA cm^{-2} (for a 1 mM solution of $\mathbf{2}^{2+}$), and no significant decrease in current was detected over five hours (Figure S9).

A catalytic rate constant of $k_{cat} = 1.14\ s^{-1}$ was calculated for $\mathbf{2}^{2+}$ using catalytic current (i_{cat}) at the first reduction potential (see the Supporting Information for details).[12a] Electrocatalysis at the first reduction potential is first order in catalyst concentration ([cat.]) as evidenced by the linear relationship between i_{cat} and [cat.] (Figure S10). Under varying concentrations of CO_2, i_{cat} increases linearly with $[CO_2]^{1/2}$ (Figure S11), confirming that catalysis is also first order in $[CO_2]$. In contrast to the previously reported parent complex ($[Ru(tpy)(bpy)(S)]^{2+}$),[12b] no saturation of the current with increasing CO_2 concentration was detected for $\mathbf{2}^{2+}$, indicating that dissociation of the CH_3CN ligand is no longer the rate limiting step in $\mathbf{2}^{2+}$. This finding is another indication for the role of the methyl substituent in promoting CH_3CN dissociation during catalysis. The normalized current ($i_{cat}/v^{1/2}$)

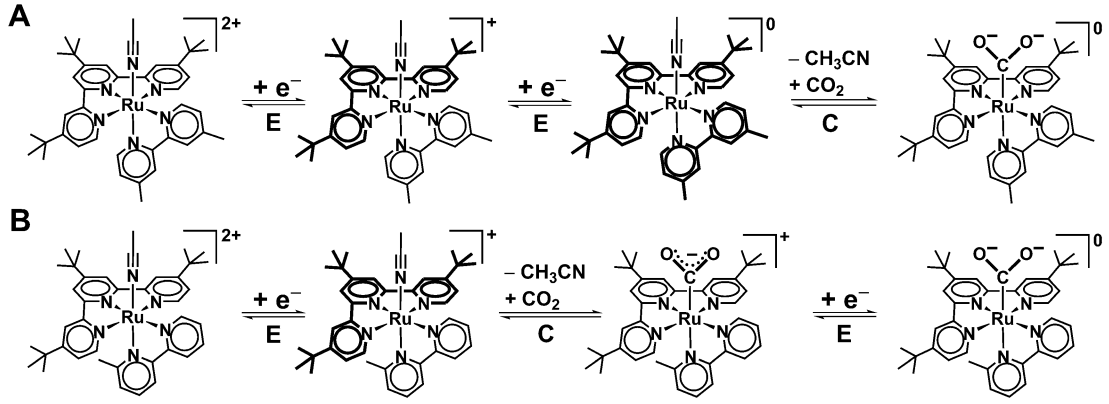

Scheme 2. Proposed initial steps for electrocatalytic CO_2 reduction by A) $\mathbf{1}^{2+}$ and B) $\mathbf{2}^{2+}$, highlighting the differences in the order of electrochemical (E) and chemical (C) steps between A) EEC and B) ECE pathways. The moieties in bold are those that are reduced.

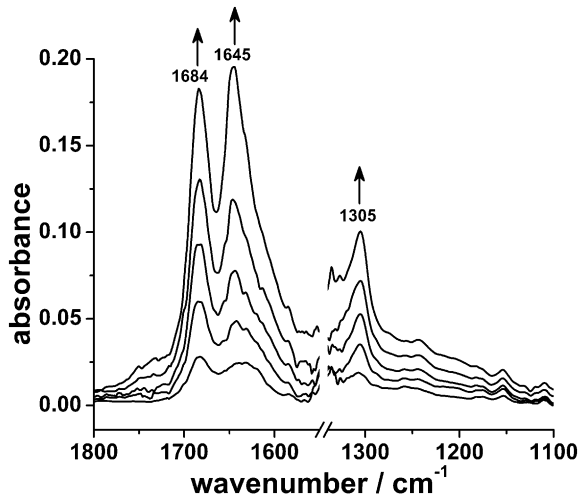

Figure 3. Changes in the IR spectrum detected during controlled potential electrolysis of $\mathbf{2}^{2+}$ at −1.82 V versus $Fc^{+/0}$ under an atmosphere of CO_2. The increase in absorbance of the three bands (1684, 1645, and 1305 cm^{-1}) arises from increasing amounts of HCO_3^- in solution that are produced during catalytic turnover at the applied potential. The arrows indicate the increase in the absorbance intensity with increasing time.

decreases with increasing scan rate (Figure S12), consistent with rate-limiting CO_2 binding at the one-electron reduced level.

Additionally, the effect of water on CO_2 reduction with $\mathbf{2}^{2+}$ was investigated. An increase in i_{cat} is detected upon increasing water content in the electrolyte solution (Figure S13). The increase in current is most likely due to water being a superior oxide acceptor.

All experiments described above are consistent with a catalytic cycle for $\mathbf{2}^{2+}$ that commences with an ECE mechanism to generate the crucial $[Ru(t\mathrm{Bu_3tpy})(6\text{-mbpy})(CO_2^{2-})]^0$ intermediate at a potential of −1.82 V versus $Fc^{+/0}$. $[Ru(t\mathrm{Bu_3tpy})(6\text{-mbpy})(CO_2^{2-})]^0$ is the catalytically active species and turns over at the same potential. Owing to the ECE mechanism, $[Ru(t\mathrm{Bu_3tpy})(6\text{-mbpy})(CO_2^{2-})]^0$ is produced at a less negative potential than in the EEC mechanism, allowing further reductions and finally catalysis to occur at an overpotential of only 0.47 V for $\mathbf{2}^{2+}$. This value is considerably lower than that found for $\mathbf{1}^{2+}$ (0.87 V)[18] and for the previously reported unsubstituted $[Ru(tpy)(bpy)S]^{2+}$,[19] both of which follow the EEC mechanism. If more negative potentials are applied (beyond −2.0 V), $\mathbf{2}^{2+}$ catalyzes CO_2 reduction by the previously reported EEC mechanism.[12b]

In summary, we have shown for the first time that incorporating a simple methyl substituent in the ligand framework can open a new mechanistic pathway for the reductive disproportionation of CO_2 to CO_3^{2-} and CO. Binding of CO_2 after the one-electron reduction of $[Ru(t\mathrm{Bu_3tpy})(6\text{-mbpy})(NCCH_3)]^{2+}$, followed by catalytic turnover at the same potential, was detected. This was supported by IR spectroscopy and GC analysis, confirming that the products, CO_3^{2-} and CO, were produced at the first reduction potential of the complex. Electron transfer from the initially reduced $t\mathrm{Bu_3tpy}$ ligand to the coordinated CO_2 enables a second electron uptake at the same potential, resulting in a compression of the reduction potentials and a decrease in the overpotential for catalysis from 0.87 V to 0.47 V. The present report is a unique example of using strategic ligand modifications to access unconventional catalytic pathways that operate at lower overpotentials. Ongoing studies are aimed at utilizing synthetic modifications within this ligand architecture to develop even more efficient electrocatalysts for CO_2 reduction.

Acknowledgements

Financial support from the Swedish Research Council, the Swedish Energy Agency, the Knut and Alice Wallenberg Foundation, and the Wenner Gren Foundation (postdoctoral stipend to T.A.W.) is gratefully acknowledged. The Swedish National Supercomputer Centre (NSC) at Linköping, Sweden, is gratefully acknowledged for providing computation time.

Keywords: carbon dioxide reduction · electrocatalysis · overpotential · reaction mechanisms · ruthenium

How to cite: *Angew. Chem. Int. Ed.* **2016**, *55*, 1825–1829
Angew. Chem. **2016**, *128*, 1857–1861

[1] a) G. A. Olah, G. K. S. Prakash, A. Goeppert, *J. Am. Chem. Soc.* **2011**, *133*, 12881–12898; b) C. Costentin, M. Robert, J.-M. Saveant, *Chem. Soc. Rev.* **2013**, *42*, 2423–2436.

[2] a) E. E. Benson, C. P. Kubiak, A. J. Sathrum, J. M. Smieja, *Chem. Soc. Rev.* **2009**, *38*, 89–99; b) N. S. Lewis, D. G. Nocera, *Proc. Natl. Acad. Sci. USA* **2006**, *103*, 15729–15735; c) M. Mikkelsen, M. Jorgensen, F. C. Krebs, *Energy Environ. Sci.* **2010**, *3*, 43–81; d) J. Qiao, Y. Liu, F. Hong, J. Zhang, *Chem. Soc. Rev.* **2014**, *43*, 631–675; e) A. M. Appel, J. E. Bercaw, A. B. Bocarsly, H. Dobbek, D. L. DuBois, M. Dupuis, J. G. Ferry, E. Fujita, R. Hille, P. J. A. Kenis, C. A. Kerfeld, R. H. Morris, C. H. F. Peden, A. R. Portis, S. W. Ragsdale, T. B. Rauchfuss, J. N. H. Reek, L. C. Seefeldt, R. K. Thauer, G. L. Waldrop, *Chem. Rev.* **2013**, *113*, 6621–6658; f) J. Schneider, H. Jia, J. T. Muckerman, E. Fujita, *Chem. Soc. Rev.* **2012**, *41*, 2036–2051; g) M. Rakowski Dubois, D. L. Dubois, *Acc. Chem. Res.* **2009**, *42*, 1974–1982.

[3] a) P. C. Ford, *Acc. Chem. Res.* **1981**, *14*, 31–37; b) D. Glasser, D. Hildebrandt, X. Liu, X. Lu, C. M. Masuku, *Curr. Opin. Chem. Eng.* **2012**, *2*, 296–302; c) A. Y. Krylova, *Kinet. Catal.* **2012**, *53*, 742–746.

[4] a) J.-M. Savéant, *Chem. Rev.* **2008**, *108*, 2348–2378; b) A. M. Appel, M. L. Helm, *ACS Catal.* **2014**, *4*, 630–633.

[5] a) M. G. I. Galinato, C. M. Whaley, D. Roberts, P. Wang, N. Lehnert, *Eur. J. Inorg. Chem.* **2011**, 1147–1154; b) C. Liu, J. N. T. Peck, J. A. Wright, C. J. Pickett, M. B. Hall, *Eur. J. Inorg. Chem.* **2011**, 1080–1093.

[6] a) M. J. Baldwin, V. L. Pecoraro, *J. Am. Chem. Soc.* **1996**, *118*, 11325–11326; b) V. K. Yachandra, K. Sauer, M. P. Klein, *Chem. Rev.* **1996**, *96*, 2927–2950; c) W. Rüttinger, G. C. Dismukes, *Chem. Rev.* **1997**, *97*, 1–24.

[7] a) S. Berardi, S. Drouet, L. Francas, C. Gimbert-Surinach, M. Guttentag, C. Richmond, T. Stoll, A. Llobet, *Chem. Soc. Rev.* **2014**, *43*, 7501–7519; b) M. D. Kärkäs, O. Verho, E. V. Johnston, B. Åkermark, *Chem. Rev.* **2014**, *114*, 11863–12001; c) X. Sala, S. Maji, R. Bofill, J. García-Antón, L. Escriche, A. Llobet, *Acc. Chem. Res.* **2014**, *47*, 504–516.

[8] a) R. M. Bullock, A. M. Appel, M. L. Helm, *Chem. Commun.* **2014**, *50*, 3125 – 3143; b) S. Tschierlei, S. Ott, R. Lomoth, *Energy Environ. Sci.* **2011**, *4*, 2340 – 2352.
[9] C. Costentin, G. Passard, M. Robert, J.-M. Savéant, *J. Am. Chem. Soc.* **2014**, *136*, 11821 – 11829.
[10] a) J. Schneider, H. Jia, K. Kobiro, D. E. Cabelli, J. T. Muckerman, E. Fujita, *Energy Environ. Sci.* **2012**, *5*, 9502 – 9510; b) E. Fujita, C. Creutz, N. Sutin, D. J. Szalda, *J. Am. Chem. Soc.* **1991**, *113*, 343 – 353; c) J. D. Froehlich, C. P. Kubiak, *Inorg. Chem.* **2012**, *51*, 3932 – 3934; d) J. D. Froehlich, C. P. Kubiak, *J. Am. Chem. Soc.* **2015**, *137*, 3565 – 3573; e) E. Fujita, L. R. Furenlid, M. W. Renner, *J. Am. Chem. Soc.* **1997**, *119*, 4549 – 4550; f) B. J. Fisher, R. Eisenberg, *J. Am. Chem. Soc.* **1980**, *102*, 7361 – 7363; g) M. Beley, J. P. Collin, R. Ruppert, J. P. Sauvage, *J. Am. Chem. Soc.* **1986**, *108*, 7461 – 7467.
[11] a) J. Hawecker, J.-M. Lehn, R. Ziessel, *J. Chem. Soc. Chem. Commun.* **1984**, 328 – 330; b) J. M. Smieja, C. P. Kubiak, *Inorg. Chem.* **2010**, *49*, 9283 – 9289; c) M. Bourrez, F. Molton, S. Chardon-Noblat, A. Deronzier, *Angew. Chem. Int. Ed.* **2011**, *50*, 9903 – 9906; *Angew. Chem.* **2011**, *123*, 10077 – 10080; d) J. M. Smieja, M. D. Sampson, K. A. Grice, E. E. Benson, J. D. Froehlich, C. P. Kubiak, *Inorg. Chem.* **2013**, *52*, 2484 – 2491; e) M. D. Sampson, A. D. Nguyen, K. A. Grice, C. E. Moore, A. L. Rheingold, C. P. Kubiak, *J. Am. Chem. Soc.* **2014**, *136*, 5460 – 5471.
[12] a) Z. Chen, C. Chen, D. R. Weinberg, P. Kang, J. J. Concepcion, D. P. Harrison, M. S. Brookhart, T. J. Meyer, *Chem. Commun.* **2011**, *47*, 12607 – 12609; b) Z. Chen, P. Kang, M.-T. Zhang, T. J. Meyer, *Chem. Commun.* **2014**, *50*, 335 – 337; c) H. Nagao, T. Mizukawa, K. Tanaka, *Chem. Lett.* **1993**, *22*, 955 – 958; d) H. Nagao, T. Mizukawa, K. Tanaka, *Inorg. Chem.* **1994**, *33*, 3415 – 3420; e) K. Tanaka, D. Ooyama, *Coord. Chem. Rev.* **2002**, *226*, 211 – 218; f) H. Konno, A. Kobayashi, K. Sakamoto, F. Fagalde, N. E. Katz, H. Saitoh, O. Ishitani, *Inorg. Chim. Acta* **2000**, *299*, 155 – 163.
[13] T. A. White, S. Maji, S. Ott, *Dalton Trans.* **2014**, *43*, 15028 – 15037.
[14] a) J. A. Ramos Sende, C. R. Arana, L. Hernandez, K. T. Potts, M. Keshevarz-K, H. D. Abruna, *Inorg. Chem.* **1995**, *34*, 3339 – 3348; b) S. Swavey, Z. Fang, K. J. Brewer, *Inorg. Chem.* **2002**, *41*, 2598 – 2607.
[15] J. D. Knoll, B. A. Albani, C. B. Durr, C. Turro, *J. Phys. Chem. A* **2014**, *118*, 10603 – 10610.
[16] P. A. Christensen, A. Hamnett, A. V. G. Muir, N. A. Freeman, *J. Electroanal. Chem.* **1990**, *288*, 197 – 215.
[17] S. C. Cheng, C. A. Blaine, M. G. Hill, K. R. Mann, *Inorg. Chem.* **1996**, *35*, 7704 – 7708.
[18] The overpotentials were calculated following previously reported methods, which employ the potential at half the catalytic current, $E_{cat/2}$, as a more precise value for the potential for catalysis. [a) See Ref. [4b]; b) J. Agarwal, T. W. Shaw, H. F. Schaefer, A. B. Bocarsly, *Inorg. Chem.* **2015**, *54*, 5285 – 5294.] The standard potential of the CO_2/CO couple in CH_3CN was taken as $E^{o}_{CO_2/CO} = -1.28$ V vs. $Fc^{+/0}$ as derived by Saveánt and co-workers and converted to $Fc^{+/0}$ using a reported value. [c) C. Costentin, S. Drouet, M. Robert, J.-M. Savéant, *Science* **2012**, *338*, 90 – 94; d) V. V. Pavlishchuk, A. W. Addison, *Inorg. Chim. Acta* **2000**, *298*, 97 – 102.].
[19] The overpotential for $[Ru(tpy)(bpy)NCCH_3]^{2+}$ was previously reported as 0.87 V. See: Ref. [18c], albeit using a somewhat different method as in this work.

Received: September 10, 2015
Revised: October 10, 2015
Published online: December 16, 2015

